Int. J. Heat Mass Transfer. Vol. 11, pp. 1795–1806. Pergamon Press 1968. Printed in Great Britain

THE EFFECT OF EXTERNAL VORTICITY ON STAGNATION-POINT HEAT TRANSFER AT HIGH PRANDTL NUMBER

S. P. SUTERA† and G. WILLIAMS‡

Center for Fluid Dynamics, Division of Engineering, Brown University, Providence, Rhode Island, U.S.A.

(*Received* 1 *January* 1968 *and in revised form* 13 *May* 1968)

Abstract—The strong sensitivity of stagnation-point heat transfer to the presence of free-stream turbulence has been attributed to vorticity amplification by stretching of vortex filaments. A mathematical model proposed by Sutera, Maeder and Kestin is examined for the case of very high Prandtl number (*Pr*). Asymptotic solutions are obtained for the limit $Pr \to \infty$. These show that the heat-transfer sensitivity continues to increase with Prandtl number. Approximately 95 per cent of the asymptotic value of the stagnation-point heat-transfer coefficient is attained at $Pr = 100$.

NOMENCLATURE

a,	constant, characteristic of plane stagnation flow;
A,	amplitude factor;
$\mathbf{c}$,	velocity vector, dimensionless;
$\mathbf{c}^*$,	velocity vector, dimensional;
c,	constant, related to wall-shear rate $[\equiv \phi''(0)/2]$;
k,	dimensionless wave number;
Pr,	Prandtl number, $= c_p\mu\kappa$;
P, Q,	constants defined after equation (23);
T,	temperature, dimensionless;
u, v, w,	dimensionless velocity components;
U, V, W,	dimensionless functions related to u, v, w;
u_n, v_n, w_n,	Fourier components of U, V, W;
x, y, z,	Cartesian coordinates (see Fig. 1).

Greek symbols

α,	dummy variable of integration, equation (20);
$\alpha_n, \beta_n, \gamma_n$,	coefficients related to the u_n, v_n, w_n, respectively;
ξ, η, ζ,	dimensionless coordinates analogous to x, y, z;
$\tilde{\eta}$,	magnified coordinate, $= Pr^{\frac{1}{3}} . \eta$;
θ_n,	Fourier components of temperature field;
Δ,	width of thermal boundary layer, a function of Pr;
γ,	incomplete gamma function;
Γ,	complete gamma function;
Σ_1, Σ_2,	sums in right members of equations (13), (14).

Subscripts

i,	summation index;
n,	Fourier index;
0,	average part (averaged over z or ζ coordinate);
w,	wall;
∞,	far from the wall;
(1),	first approximation;
(2),	second approximation.

† Member of Am. Soc. Mech Engrs. Present address: Dept. of Mechanical and Aerospace Engineering, Washington University, St. Louis, Missouri, U.S.A.

‡ Research Assistant.

INTRODUCTION

SOME recent theoretical work [1, 2] has suggested that vorticity amplification due to stretching could be the predominant mechanism underlying the strong sensitivity of stagnation-point heat transfer to free-stream turbulence. Calculations were made using a simplified mathematical model which showed that vorticity of sufficiently large scale and appropriately oriented can be amplified as it is convected into the stagnation-point boundary layer. This amplification can induce substantial three-dimensional effects in the neighborhood of the stagnation point and it was found that the mean temperature profile is much more responsive to these effects than the mean velocity profile. As a consequence, relatively large increases in the wall-heat-transfer rate were calculated under conditions which changed the mean wall-shear rate by insignificant amounts. For example, added vorticity which increased the wall-shear rate by less than 3 per cent augmented the wall-heat-transfer rate by as much as 40 per cent.

In the course of these same calculations the influence of Prandtl number on the sensitivity of the thermal boundary layer was investigated. The heat-transfer problem was solved [2] for $Pr = 0{\cdot}70$, 7·0 and 100 and the results revealed the influence of Prandtl number to be significant. Among these three cases the sensitivity was found to be greatest for $Pr = 7{\cdot}0$ and least for $Pr = 100$. This implies the existence of a Prandtl number for which the sensitivity is maximum as well as a disappearance of the effect in fluids of very large Prandtl number. On physical grounds this finding appeared plausible. It was argued that, as the Prandtl number increases, the energy transfer takes place in an increasingly narrow region adjacent to the boundary. The velocity field being assumed independent of Prandtl number, the distortions provoked in it by the added vorticity eventually reach their maximum values outside the thermal boundary layer and might not, then, be able to noticeably affect the latter.

To examine the validity of this physical argument as well as the result previously calculated, it was decided to perform an asymptotic analysis of the mathematical model for $Pr \to \infty$. The asymptotic analysis showed that the sensitivity of the stagnation-point heat transfer to added vorticity continues to increase with the Prandtl number. Hence, the physical argument outlined above is not borne out and the results computed previously [2] for the case $Pr = 100$ were not corroborated. Subsequently, Williams [3] performed extensive independent computations based on the vorticity amplification model and reexamined, in particular, the influence of Prandtl number. Utilizing the Continuous System Modeling Program (CSMP) developed by the IBM Corporation for its 1130 Digital Computer, Williams computed the cases $Pr = 0{\cdot}70$, 2·70, 2·85, 3·00, 7·00 and 100. His result for $Pr = 100$, when properly normalized, lies within 5 per cent of the asymptotic value. In fact, the result for $Pr = 7$ differs by only 15 per cent from the $Pr = \infty$ case, which shows that the Prandtl number influence is strongest for $Pr < 7$. The asymptotic analysis, reinforced by the independent computations of Williams, points to the conclusion that Sutera's previous computation for the case $Pr = 100$ [2] was erroneous.

This paper describes the asymptotic analysis and presents numerical results based thereon for the velocity field computed by Williams [3]. Williams' heat-transfer results for Prandtl numbers 0·7, 7 and 100 are presented also for comparison.

RELATED WORK

Analytical

The literature contains many contributions on the forced convection energy equation for laminar boundary flows at high Prandtl numbers. The basic one was made by Lighthill [4] who used the von Mises' transformation to derive a general expression for the rate of heat transfer at the solid surface. Acrivos [5] later published the complete solution of the appropriate partial differential equation governing the constant-property case when dissipation is negligible and the surface is isothermal.

His result is general enough to cover the simple (no added vorticity) stagnation-point boundary layer which forms the basis for the present analysis. In this case, however, the presence of distorting influences in the equations governing both the velocity and the temperature fields makes it expedient to work out the necessary magnification of the independent variable *ab initio*. It will be seen that this step is quite straightforward.

Experimental

There is much experimental evidence attesting to the considerable influence of free-stream turbulence on stagnation-point heat transfer in flows of air. See, for example, the paper by Kestin, Maeder and Sogin [6]. Data on the analogous situation in higher Prandtl number fluids is quite meager. The results of an experimental investigation of forced convective heat transfer from a cylinder to water in crossflow in the Reynolds number range 10^4–10^5 was published recently by Fand [7]. On the basis of his data this author gives two correlations for average heat transfer of the form $\overline{Nu}_f(Re_f, Pr_f)$, the subscript f signifying that fluid properties are evaluated at the arithmetic mean film temperature. These correlations are compared to an analogous one proposed by Perkins and Leppert [8, 9] on the basis of measurements at Reynolds numbers from 40 to 10^5 and Prandtl numbers from 1 to 300. Nusselt numbers predicted by the latter correlation are about 65 per cent higher than those calculated from Fand's equations.

Perkins and Leppert also made local heat-transfer measurements on uniformly heated cylinders to water in crossflow [9]. The experimental data taken in the laminar region were found to be as much as 20 per cent higher than predictable analytically. Perkins and Leppert attributed this disparity to the influence of free-stream turbulence which they estimated had an intensity of about 1 per cent. Measurements taken with a constant temperature hot-film anemometer, however, indicated an average turbulence level of $2{\cdot}9 \pm 0{\cdot}5$ per cent. The authors charged this difference to the possible effect of the walls in their relatively narrow test section. Perkins and Leppert did place screens upstream of the test cylinder to break up large scale turbulence.

Fand [7] did not measure turbulence level in his experiments but assumes that it was much lower than in the flow of Perkins and Leppert. He opines, nevertheless, that turbulence could not account for the 54–76 per cent difference between the predictions of his correlations and that of Perkins and Leppert. The theoretical work presented below predicts that the sensitivity of *local* heat-transfer rates is intensified at high Prandtl numbers. This prediction plus the enormous effects measured in air flows [6] suggest that turbulence could indeed be the answer.

At Brown University research on this effect has shifted in emphasis to experimental verification of the vorticity amplification idea. Very recently Sadeh, Sutera and Maeder [10] reported turbulence measurements made in the vicinity of a two-dimensional stagnation point which support strongly the major predictions of the theoretical vorticity-amplification model. Among these is the existence of a neutral scale for vorticity dividing those scales which are amplified as they approach the stagnation point from those which decay steadily. The neutral scale observed in the experiments was in excellent agreement with the theoretical value. Also, a consistent spatial periodicity in the mean velocity field near the wall along a direction normal to the plane of the average stagnation flow was detected. This periodicity, suggestive of an array of vortices with axes parallel to the mean streamline direction near the wall, was also predicted by the theory [1, 2]. The average shear stress at the wall, determined from boundary-layer velocity profiles, was found to increase with the turbulence intensity measured at the outer edge of the boundary layer, thus on the amount of amplification experienced by the turbulence from its free-stream value. At this writing no complementary measurements of wall-heat-transfer rate have yet been attempted.

MATHEMATICAL PROBLEM

The relevant differential equations and boundary conditions are taken directly from [1, 2] without change in notation. Although a brief description of the notation and the equations is essential to the coherence of this paper, a thorough discussion of their development and the physical ideas underlying the mathematical model would be uneconomical here. For this the interested reader must be referred to the original papers. Furthermore, since the Prandtl number effect, which is the main interest here, does not affect the velocity field, because of the constant-properties assumption, only the equations governing the temperature field will be emphasized. In fact, the particular velocity field will be treated as known and taken from [3] where it was calculated.

Figure 1 shows the physical situation and the

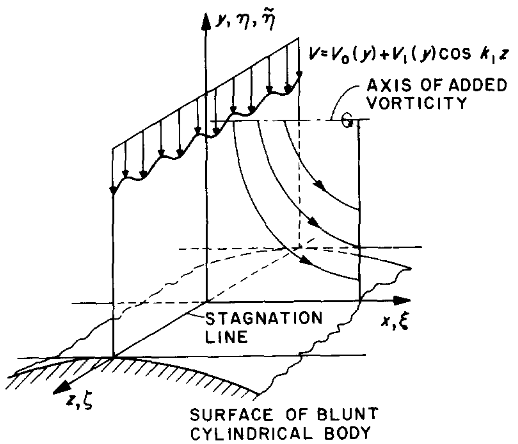

FIG. 1. Physical situation and coordinate system.

coordinate system. It depicts a steady flow of a viscous, incompressible fluid having constant properties into a plane stagnation point. The problem is identical to the classical Hiemenz problem but for the addition of vorticity in the form of a simple sinusoidal variation imposed on the y-component of velocity. Other simplifying restrictions imposed are complete time-independence, incompressibility and negligible viscous dissipation.

The question is often raised as to how such a time-independent flow can be called a valid representation of a turbulent flow which is intrinsically unsteady. In response it must be emphasized that the turbulent flows of interest here are steady on the average and convect three-dimensional vorticity with a continuous spectrum of eddy size. Since the turbulent eddies move with the average flow, the real flow field fluctuates with time at any fixed point. However, the importance of this unsteadiness alone, unaccompanied by the vortex-stretching mechanism, has been dispelled by careful analyses. For example, Kestin, Maeder and Wang [11] showed that small harmonic oscillations superimposed on a steady flow caused only second-order changes in the skin friction and heat transfer. Furthermore, the turbulence studies reported in [10] show a clear similarity between the time-averaged properties of a real turbulent flow and the steady, but vorticity-bearing flow of the theoretical model.

Governing equations and boundary conditions

The problem is phrased in terms of dimensionless variables defined by the following expressions, wherein the dimensional dependent variables are designated by an asterisk superscript:

(a) the co-ordinates

$$\xi, \eta, \zeta = (a/\nu)^{\frac{1}{2}}x, (a/\nu)^{\frac{1}{2}}y, (a/\nu)^{\frac{1}{2}}z;$$

(b) the velocity vector

$$\mathbf{c} \equiv (a\nu)^{-\frac{1}{2}}\,\mathbf{c}^*$$

(c) the temperature

$$T \equiv (T_w - T^*)/(T_w - T_\infty).$$

In these definitions the subscripts w and ∞ denote conditions at the wall and very far from the wall ($y, \eta \to \infty$), respectively, ν is the kinematic viscosity and a is a constant characteristic of the stagnation flow with dimensions of reciprocal time. This constant comes from the conditions on the tangential and normal velocity components (x and y or ξ and η components) at the outer edge of the boundary layer, viz.

$$u^* \to ax, v^* \to -ay + \text{const.}$$

as $\eta \to \infty$. In terms of the unbounded potential flow past a circular cylinder of diameter D, $a = 4V_\infty/D$.

In the original work [1, 2] the governing equations were taken to be the time-independent vorticity-transport equation, the incompressible continuity equation and the time-independent energy-transport equation with no dissipation term. Only the third of these will be treated here. In dimensionless form it is

$$(\mathbf{c}\,.\,\nabla)T = (1/Pr)\,\nabla^2 T. \qquad (1)$$

The boundary conditions on T are

$$T(\xi, 0, \zeta) = 0, \qquad (2)$$

$$T \to 1 \quad \text{as} \quad \eta \to \infty. \qquad (3)$$

The velocity and temperature fields were restricted to possess the same underlying similarity as the Hiemenz flow field as indicated by the following forms:

$$\left.\begin{aligned} u &= U(\eta, \zeta)\,.\,\xi, \\ v &= V(\eta, \zeta), \\ w &= W(\eta, \zeta), \\ T &= T(\eta, \zeta). \end{aligned}\right\} \qquad (4)$$

Fourier structure specification

Vorticity addition was accomplished by superposing a simple sinusoidal variation on the normal or η velocity component far from the boundary; thus

$$V(\eta, \zeta) \to V_0(\eta) + V_1(\eta)\cos k\zeta \quad \text{as} \quad \eta \to \infty, \quad (5)$$

where V_1/V_0 was required to be small fraction at large values of η.

Because the equations governing the velocity field are nonlinear, excitation of the boundary-layer system by a simple harmonic waveform will cause ultra-harmonic components to be generated. For this reason a complete Fourier structure was assumed for each of the dependent variables listed in equation (4). In particular

$$T = T_0(\eta) + A \sum_{n=1}^{\infty} \theta_n(\eta)\cos k_n\zeta. \qquad (6)$$

The factor A is called the amplitude parameter and represents the maximum amplitude attained by the imposed sinusoidal velocity variation, equation (5). In drawing a comparison between the steady distributed vorticity of this model and the vorticity in a real turbulent flow, the factor A is analogous to the R.M.S. value of the local turbulent fluctuations, thus to the local turbulence intensity, in the vicinity of the maximum value attained by these fluctuations. In the course of the computations [1–3] A was used as an adjustable parameter for controlling the strength of the added vorticity, as indicated by the change produced in the wall shear rate.

The k_n are dimensionless wave numbers, positive, not necessarily integers but ordered according to $k_n = nk_1$, $n = 1, 2, \ldots$. An important conclusion drawn from this model [1] was that vorticity amplification can occur only if the imposed vorticity scale, as represented by its wavelength, is larger than a certain neutral scale which is indicated by the theory. In terms of the wave number k_1, it is necessary that $k_1 < 1$ for amplification. In [1] the calculations were performed for the neutral scale $k_1 = 1$ and in [2] for $k_1 = \frac{2}{3}$. Williams [3] took $k_1 = \frac{3}{5}$. The asymptotic analysis to follow will take $k_1 = \frac{3}{5}$ and thus will be directly comparable to Williams' work. The velocity field calculated therein will be taken directly as a known input.

Resulting ordinary differential equations

From [2] come the differential equations which govern the average part T_0 of the temperature field and the harmonic components θ_n of the periodic part:

$$\frac{1}{Pr} T_0'' + \phi T_0' = \tfrac{1}{2}A^2 \sum_{i=1}^{\infty} \{u_i\theta_i + (v_i\theta_i)'\} \tag{7}$$

$$\frac{1}{Pr}(\theta_n'' - k_n^2\theta_n) + \phi\theta_n' = T_0' v_n + \tfrac{1}{2}A \sum_{i=1}^{\infty} \times \{[v_i(\theta_{n+i} + \theta_{i-n} + \theta_{n-i})]' + u_i(\theta_{n+i} + \theta_{i-n} + \theta_{n-i}) - (n/i)\, w_i(\theta_{n+i} - \theta_{i-n} - \theta_{n-i})\}, \tag{8}$$

where the prime notation means differentiation with respect to η. The u_i, v_i, w_i are the harmonic components of the velocity functions U, V, W introduced in equation (4). In the summations i is a dummy index and quantities which have subscripts such as $n - i$ are to be replaced by zero whenever their subscripts are zero or negative.

The function $\phi(\eta)$ is derived from the continuity equation and represents both $U_0(\eta)$ and $V_0(\eta)$, the average parts of $U(\eta)$ and $V(\eta)$, according to

$$\phi \equiv -V_0, \qquad U_0 = \phi'. \tag{9}$$

Note that equation (7) is a single equation while equation (8) represents an infinite set since $1 \leqslant n < \infty$. These equations are all linear but coupled in a complicated manner.

The boundary conditions which the solutions to equations (7) and (8) must satisfy are

$$T_0(0) = \theta_n(0) = 0, \qquad T_0 \to 1, \theta_n \to 0 \quad \text{as} \quad \eta \to \infty. \tag{10}$$

ASYMPTOTIC SOLUTION FOR LARGE *Pr*

Asymptotic solutions to equations (7) and (8), subject to the conditions (10), are sought for large Pr, specifically for $Pr \to \infty$. The governing equations show clearly that this is a singular perturbation problem; a small parameter (Pr^{-1}) multiplies the highest derivatives in the differential equations. As a consequence these derivatives would be lost in any straightforward perturbation scheme, the order of the equations would be reduced (to the first) and two boundary conditions could not be enforced.

The physical significance of these remarks is clear. When $Pr \gg 1$ the thermal boundary layer will be much thinner than the velocity boundary layer. In the limit $Pr = \infty$ the former collapses to zero thickness. In order to treat this problem of a boundary layer within a boundary layer mathematically, it is necessary to find an appropriate coordinate magnification, which is linked to the parameter Pr and maintains the width of the thermal boundary layer at order unity. The magnification must also maintain the order of the second derivative at a level comparable to the other terms in the equations and thereby preserve the true second-order nature of the equations.

The singular perturbation problem may also be phrased in terms of the method of matched asymptotic expansions, according to which the usual boundary-layer analysis provides the leading term of an asymptotic expansion. This would be useful to do if further terms in the expansion were desired; the intention here, however, is to calculate only the leading term. Hence, the discussion to follow will not adhere strictly to the formalism of the method of matched expansions but some allusions to the ideas will occur naturally. For example, it can be shown that the outer boundary conditions, equation (10), represent exactly the leading terms of suitable outer expansions for T_0 and the θ_n. These leading terms correspond to solutions of equations (7) and (8) with $Pr = \infty$.

Approximate expressions for the velocity field

Because the domain of interest on the η scale is a very narrow one beginning at $\eta = 0$, the various components of the velocity field may be represented by the first nonzero terms of their respective Maclaurin's series in powers of η. The error associated with such representations increases with the extent of the domain of interest, but is calculable since the velocity field is known in principle.

In reality, only an incomplete knowledge of the velocity field is possessed because the three infinite sets of harmonic components (u_n, v_n, w_n) could never be calculated completely. This lack of a complete knowledge of the velocity field is inconsequential, however, for the particular case of interest, viz. $k_1 = \frac{3}{5}$, $A \leqslant 3$. The computations performed in [2, 3] confirm that for this range of A the second-harmonics, u_2, v_2, w_2, were about an order of magnitude smaller than their first-harmonic counterparts. By means of inductive reasoning it could also be seen that the whole set of Fourier components tailed off very rapidly so that, for practical purposes, harmonics higher than the second could be ignored.

The general properties of the velocity field are such that, for small η,

$$\begin{aligned} \phi &= c\eta^2 + O(\eta^3), & c &\equiv \tfrac{1}{2}\phi''(0), \\ u_n &= \alpha_n\eta + O(\eta^2), & \alpha_n &\equiv u_n'(0), \\ v_n &= \beta_n\eta^2 + O(\eta^3), & \beta_n &= \tfrac{1}{2}v_n''(0), \\ w_n &= \gamma_n\eta + O(\eta^2), & \gamma_n &\equiv w_n'(0). \end{aligned} \tag{11}$$

Coordinate magnification

Coordinates of order unity in the thermal boundary layer region are obtained by magnifying the coordinate η. (It is worthwhile to recall that η is already a magnified boundary-layer coordinate, its magnification factor $\nu^{-\frac{1}{2}}$ being appropriate for the velocity boundary layer.) Let the width of this region be of order $\Delta(Pr)$, where Δ is a function which vanishes as $Pr \to \infty$. Then an appropriate magnified coordinate is

$$\tilde{\eta} = \eta/\Delta(Pr). \tag{12}$$

The stretching factor $1/\Delta(Pr)$ is to be determined from the governing differential equation [(7) or (8)]. It is clear that no magnification is necessary for the dependent variable T_0 which is of order unity inside the boundary layer. The θ_n representing part of the same temperature field cannot be measured on a different scale from T_0 and, hence, receive no magnification.

Substitution of the approximate forms, equations (11), into equations (7) and (8), followed by the change of independent variable, equation (12), gives, after dividing through each equation by Δ,

$$\frac{1}{Pr\,.\,\Delta^3}T_0'' + c\tilde{\eta}^2T_0' = \frac{\Delta^2}{2}\sum_{i=1}^{\infty}\left[\alpha_i\tilde{\eta}\theta_i + (\beta_i\tilde{\eta}^2\theta_i)'\right] + O(\Delta), \tag{13}$$

$$\begin{aligned} \frac{1}{Pr\,.\,\Delta^3}\theta_n'' - \frac{k_n^2}{Pr\,.\,\Delta}\theta_n + c\tilde{\eta}^2\theta_n' = \beta_i\tilde{\eta}^2T_0' \\ + \frac{\Delta}{2}\sum_{i=1}^{\infty}\Big[\{\beta_i\tilde{\eta}^2(\theta_{n+i} + \theta_{i-n} + \theta_{n-i})\}' \\ + \alpha_i\tilde{\eta}(\theta_{n+i} + \theta_{i-n} + \theta_{n-i}) \\ - \frac{n}{i}\gamma_i\tilde{\eta}(\theta_{n+i} - \theta_{i-n} - \theta_{n-i})\Big] + O(\Delta). \end{aligned} \tag{14}$$

In these two equations the prime signifies differentiation with respect to $\tilde{\eta}$.

The factor Δ is determined from either of equations (13) and (14) by considering the limit $Pr \to \infty$ with $\tilde{\eta}$ fixed. Only the coefficients containing Δ are affected by this limiting process. The one multiplying the highest derivatives T_0'' and θ_n'', or more precisely the

$$\lim_{Pr\to\infty}\left[\frac{1}{Pr\,.\,\Delta^3}\right]$$

determines Δ. This limit may be zero, infinite or finite. The first two possibilities would mean degenerate solutions incapable of satisfying the inner boundary conditions, $T_0(0) = 0$, $\theta_n(0) = 0$, and matching the outer flow $T_0x = 1$, $\theta_n = 0$ as $\tilde{\eta} \to \infty$. Only the finite limit is of interest and the simplest choice for the constant limit is unity. Hence

$$\Delta(Pr) = Pr^{-\frac{1}{3}} \quad \text{and} \quad \tilde{\eta} = Pr^{\frac{1}{3}}\eta. \tag{15}$$

Accordingly the coefficient of θ_n in equation (14) vanishes as $Pr^{-\frac{2}{3}}$ in the limit $Pr \to \infty$.

Resulting equations

Equations (13) and (14) now become

$$T_0'' + c\tilde{\eta}^2T_0' = \tfrac{1}{2}\Delta^2\Sigma_1, \tag{16}$$

$$\theta_n'' + c\tilde{\eta}^2\theta_n' = \beta_n\tilde{\eta}^2T_0' + \tfrac{1}{2}\Delta\Sigma_2, \tag{17}$$

where, for brevity, Σ_1 and Σ_2 designate the sums. It is interesting to note that the functions T_0 and θ_n will have the same complementary solutions. Furthermore, since the wave number

k_n does not appear in equation (17) it is expected that all the θ_n will be similar in form, differing only in amplitude. To repeat, the boundary conditions to be satisfied are

$$\begin{aligned} &T_0(0) = \theta_n(0) = 0, \\ &T_0 \to 1, \quad \theta_n \to 0 \quad \text{as} \quad \tilde{\eta} \to \infty. \end{aligned} \tag{18}$$

Solution by successive approximations

Solutions of equations (16) and (17) was effected by the same method of successive approximation and iteration applied in [1, 2]. The process is begun by neglecting the spectral interaction functions represented by Σ_1 and Σ_2. Then it is possible to solve for a first approximation to T_0, call it $T_{0(1)}$, which may then be used in equation (17) to solve for first approximations to the θ_n. The $\theta_{n(1)}$ may then be used to approximate Σ_1 in equation (16). The next step is to calculate a second approximation for T_0. In the calculation discussed below no iteration was performed beyond this step.

Accordingly, the first approximation to T_0 satisfies the following differential equation and boundary conditions:

$$\begin{aligned} &T''_{0(1)} + c\tilde{\eta}^2 T'_{0(1)} = 0, \\ &T_{0(1)}(0) = 0, \qquad T_{0(1)} \to 1 \quad \text{as} \quad \tilde{\eta} \to \infty. \end{aligned} \tag{19}$$

The solution is

$$T_{0(1)}(\tilde{\eta}) = \frac{3}{\Gamma(\frac{1}{3})}\left(\frac{c}{3}\right)^{\frac{1}{3}} \int_0^{\tilde{\eta}} \exp\left(-\frac{c}{3}\alpha^3\right) \mathrm{d}\alpha$$

$$= \frac{\gamma\left(\frac{1}{3}, \frac{c}{3}\tilde{\eta}^3\right)}{\Gamma(\frac{1}{3})}. \tag{20}$$

This will be recognized as the incomplete gamma function of $\frac{1}{3}$ and has been tabulated by Pearson [12].

The first approximations to the θ_n satisfy

$$\begin{aligned} &\theta''_{n(1)} + c\tilde{\eta}^2\theta'_{n(1)} = \beta_n\tilde{\eta}^2 T'_{0(1)}, \\ &\theta_{n(1)}(0) = 0, \qquad \theta_{n(1)} \to 0 \quad \text{as} \quad \tilde{\eta} \to \infty. \end{aligned} \tag{21}$$

The complete solutions:

$$\theta_{n(1)} = -\frac{\beta_n}{\Gamma(\frac{1}{3})\,3^{\frac{1}{3}}c^{\frac{2}{3}}} \cdot \tilde{\eta} \exp\left(-\frac{c}{3}\tilde{\eta}^3\right). \tag{22}$$

With these solutions and the approximate forms for u_n, v_n and w_n, equations (11), a first approximation can be obtained for the right member of equation (16). In abbreviated notation the second approximation $T_{0(2)}$ is governed by

$$T''_{0(2)} + c\tilde{\eta}^2 T'_{0(2)} = A^2(P + Q\tilde{\eta}^3)\tilde{\eta}^2 \exp\left(-\frac{c}{3}\tilde{\eta}^3\right), \tag{23}$$

where

$$P \equiv \frac{-1}{2\,.\,3^{\frac{1}{3}}c^{\frac{2}{3}}\Gamma(\frac{1}{3})} \sum_{i=1}^{\infty} (\alpha_i + 3\beta_i)\beta_i,$$

and

$$Q \equiv \frac{c^{\frac{1}{3}}}{2\,.\,3^{\frac{1}{3}}\,\Gamma(\frac{1}{3})} \sum_{i=1}^{\infty} \beta_i^2.$$

The boundary conditions to be satisfied by $T_{0(2)}$ are the same as those satisfied by $T_{0(1)}$, equation (19).

The general solution for $T_{0(2)}$ is

$$T_{0(2)} = \frac{\gamma\left(\frac{1}{3}, \frac{c}{3}\tilde{\eta}^3\right)}{\Gamma(\frac{1}{3})} - A^2\left\{\left(\frac{P}{3c} + \frac{2Q}{3c^2}\right)\tilde{\eta} + \frac{Q}{6c}\tilde{\eta}^4\right\} \exp\left(-\frac{c}{3}\tilde{\eta}^3\right). \tag{24}$$

This form clearly displays the contribution of added vorticity, represented by the terms multiplied by A^2.

Wall-heat-transfer rate

The heat-transfer rate at the wall is proportional to the quantity $T'_0(0)$. Differentiation of equation (24) followed by evaluation at $\tilde{\eta} = 0$ yields

$$T'_{0(2)}(0) = \frac{3^{\frac{2}{3}}c^{\frac{1}{3}}}{\Gamma(\frac{1}{3})} - A^2\left(\frac{P}{3c} + \frac{2Q}{3c^2}\right). \tag{25}$$

The first member on the right represents the rate corresponding to the simple Hiemenz boundary layer ($A = 0$) and the term in A^2 is the contribution of the added vorticity. It will be seen shortly that the latter is positive, meaning that the added vorticity increases the heat transfer. It should be remembered that the derivative of equation (25) is taken with respect to the stretched variable $\tilde{\eta}$. Multiplication of this result by $Pr^{\frac{1}{3}}$ gives the wall gradient in terms of the original variable η since

$$\frac{dT_0}{d\eta} = \frac{dT_0}{d\tilde{\eta}} \cdot \frac{d\tilde{\eta}}{d\eta} = \frac{dT_0}{d\tilde{\eta}} \cdot Pr^{\frac{1}{3}}. \qquad (26)$$

It is interesting to note that $dT_0/d\eta$, evaluated at $\eta = 0$, is precisely the Nusselt number based on the viscous length $\sqrt{\nu/a}$.

Numerical results

In order to calculate temperature profiles from equations (20), (22) and (24) the constants c, α_i and β_i must be obtained from a previously solved velocity field. This information is taken from [3] where, for reasons explained above, only the first and second harmonic components of the periodic portion of the velocity field were computed. The pertinent numbers are listed in Table 1 for four values of the amplitude parameter A.

It is worthwhile repeating that these numbers were computed for the case $k_1 = \frac{3}{5}$. The amplitudes of the first harmonics, α_1, β_1, are independent of A, by virtue of their normalized definition, but the ratios α_2/α_1, β_2/β_1 are proportional to A. The small values of these ratios is clearly evident from the preceding tabulation.

By means of equations (22) and (24) profiles of

$$\theta_{n(1)} \Big/ \left(- \frac{\beta_n}{\Gamma(\frac{1}{3})\, 3^{\frac{1}{3}} c^{\frac{2}{3}}} \right) = \tilde{\eta} \exp\left(- \frac{c}{3} \tilde{\eta}^3 \right)$$

and $T_{0(2)}$ were computed and are shown plotted in Figs. 2 and 3. Only one curve, corresponding to $A = 1$, is given for $\theta_{n(1)}$ since the maximum deviation from this curve, for values of $A \leqslant 3$, is only about 0·04 unit. It can be seen in Fig. 2 that the harmonic components of the

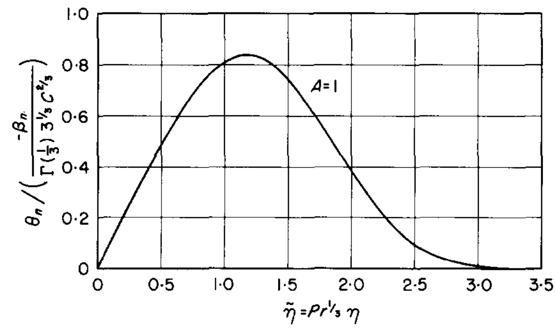

FIG. 2. Asymptotic solution for high Prandtl number. First approximation to harmonic components of the temperature function.

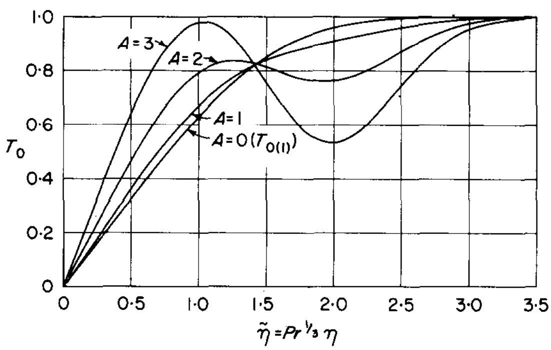

FIG. 3. Asymptotic solution for high Prandtl number. First approximation ($A = 0$) and second approximations ($A = 1, 2, 3$) for mean temperature field T_0. $T_{0(1)}$ corresponds to basic two-dimensional flow without added vorticity.

Table 1

	$A = 0$	1	2	3
$c = \frac{1}{2}\phi''(0)$	0·6163	0·6206825	0·633744	0·655231
$\alpha_1 = u_1'(0)$	0	−0·0917220	−0·0917220	−0·0917220
$\alpha_2 = u_2'(0)$	0	−0·008033	−0·016066	−0·024099
$\beta_1 = \frac{1}{2}v_1''(0)$	0	0·93965	0·93965	0·93965
$\beta_2 = \frac{1}{2}v_2''(0)$	0	−0·0652368	−0·1304736	−0·1957104

Table 2. Sensitivity of wall-heat-transfer rate to added vorticity at various Prandtl numbers
Table entries are values of $T'_0(0)/Pr^{\frac{1}{3}}$
(Changes from the value at $A = 0$ shown in parentheses)

	Analog computations of Sutera [2] $k_1 = \frac{2}{3}$			Digital computations of Williams [3] $k_1 = \frac{3}{5}$			Asymptotic analysis $k_1 = \frac{3}{5}$
A	$Pr = 0.70$	7·0	100	0·70	7·0	100	∞
0	0·574	0·640	0·672	0·558	0·615	0·643	0·661
0·5	0·581	0·653	0·677	0·565	0·630	0·660	
	(1·2 %)	(2·0 %)	(0·7 %)	(1·2 %)	(2·4 %)	(2·6 %)	
1·0	0·599	0·685	0·686	0·585	0·673	0·713	0·739
	(4·3 %)	(7·0 %)	(2·0 %)	(4·8 %)	(9·4 %)	(10·8 %)	(11·8 %)
1·5				0·620	0·745	0·799	
				(11·1 %)	(21·1 %)	(24·2 %)	
2·0	0·670	0·812	0·721	0·668	0·846	0·922	0·968
	(16·7 %)	(26·8 %)	(7·2 %)	(19·7 %)	(37·5 %)	(43·3 %)	(46·4 %)
2·5	0·721	0·897		0·730	0·975	1·078	
	(25·6 %)	(40·1 %)		(30·8 %)	(58·5 %)	(67·6 %)	
3·0	0·791			0·806	1·133	1·270	1·334
	(37·8 %)			(44.4 %)	(84·2 %)	(97·5 %)	(101·8 %)

periodic part of the temperature field reach their maxima very near the mid-point of the thermal boundary layer. The concomitant distortion of the average (over the z-coordinate) temperature field, to second approximation, Fig. 3, is always such as to increase the temperature gradient at the wall, thus improving the wall-heat-transfer rate. It should be noted that the profile labeled $A = 0$ is the profile corresponding to perfectly two-dimensional flow, i.e. a flow with no added vorticity.

The wall-heat-transfer rates for $A = 0$ to $A = 3$ were also computed. These are tabulated in the extreme right-hand column of Table 2.

Table 2 also summarizes the Prandtl number influence for the three cases computed in [2, 3]. (In this table, the prime always means $d/d\eta$ and per cent changes, listed in parentheses beneath the table entries, are referred to the values at $A = 0$.) For the case $Pr = 100$ and *no added vorticity* ($A = 0$) the asymptotic analysis gives $T'(0) = 3{\cdot}07$, differing by about 3 per cent from the exact 2·9856 obtained on the digital computer. In fact, even for a Prandtl number as low as 7·0, the corresponding difference is of the order of 7 per cent.

Comparison of the increments in $T'_0(0)$ predicted by the asymptotic analysis (last column on the right) on the one hand and those computed for $Pr = 100$ on the other gives evidence to the discrepancy mentioned in the Introduction. There seems to be no physical basis to justify both a maximum and a minimum in the increment dependence on Pr. Hence, we must conclude that the $Pr = 100$ case calculated in [2] is in error.

CONCLUSIONS

The calculation described above is intended to demonstrate the sensitivity of heat transfer in the plane stagnation flow to the presence of vorticity susceptible to amplification by stretching when the Prandtl number is very high. The results tabulated in Table 2 show that the percentage increase in the wall-heat-transfer rate is greater in this case than for all lower Prandtl numbers previously calculated [2, 3].

In the Introduction to this paper a plausible argument, used previously to justify the inverse effect of Prandtl number on heat-transfer sensitivity, was outlined briefly. In the light of the contrary prediction given by the asymptotic analysis and its verification by more accurate computations, it is appropriate to ask where a fallacy in the physical argument might lie. Equation (7) governing the function T_0 and the approximate solutions, equation (22), for the θ_n give the answer. First, it must be noted that the right member of equation (7) contains products involving not only the θ_n but also the slopes of these functions. The asymptotic analysis has shown that within the thermal boundary layer, which is $O(Pr^{-\frac{1}{3}})$ in width, the θ_n are $O(\beta_n)$ while the slopes $d\theta_n/d\eta$ are $O(\beta_n v\, Pr^{\frac{1}{3}})$. Consequently, the terms $u_i\theta_i$ and $(v_i\theta_i)'$ are $O(\alpha_n\beta_n Pr^{-\frac{1}{3}})$ and $O(\beta_n^2 Pr^{-\frac{1}{3}})$ respectively. Because of the decreasing nature of the coefficients α_n and β_n and their relative magnitudes the leading contribution is actually due to the term $(v_1\theta_1)'$ which is $O(\beta_1^2 Pr^{-\frac{1}{3}})$ or simply $O(Pr^{-\frac{1}{3}})$ because β_1^2 is of order unity. It is easy to show that the two terms of the left member of equation (7) are also $O(Pr^{-\frac{1}{3}})$. Thus the leading contribution of the right member, which represents the effect of the added vorticity on the mean temperature profile, is of the same order in Pr as the other terms in the differential equation. Therefore, in the limit $Pr \to \infty$, this contribution does not become less important than the others with the result that the sensitivity to the added vorticity persists and, in fact, increases.

ACKNOWLEDGEMENTS

The work described in this paper constitutes part of a cooperative research program on heat transfer in unsteady flows of the Aeronautical Research Laboratories, Office of Aerospace Research of the U.S. Air Force, under the technical supervision of Dr. M. Scherberg (Contract No. F 33615 67 c 1754). This support together with partial support from Grant GK-575 from the National Science Foundation is gratefully acknowledged.

REFERENCES

1. S. P. Sutera, P. F. Maeder and J. Kestin, On the sensitivity of heat transfer in the stagnation-point boundary layer to free-stream vorticity, *J. Fluid Mech.* **16**, 497–520 (1963).
2. S. P. Sutera, Vorticity amplification in stagnation-point flow and its effect on heat transfer, *J. Fluid Mech.* **21**, 513–534 (1965).
3. G. Williams, Enhancement of heat and mass transfer in a stagnation region by free stream vorticity, MS. thesis, Division of Engineering, Brown University (1968); see also G. Williams, Enhancement of heat and mass transfer in a stagnation region by free stream vorticity, Brown University T.R. No. AF 1754/1 (October 1967).
4. M. J. Lighthill, Contribution to the theory of heat transfer through a laminar boundary layer, *Proc. R. Soc.* **A202**, 359–377 (1950).
5. A. Acrivos, Solution of the laminar boundary layer energy equation at high Prandtl numbers, *Physics Fluids* **3**, 657–658 (1960).
6. J. Kestin, P. F. Maeder and H. H. Sogin, The influence of turbulence on the transfer of heat to cylinders near the stagnation point, *Z. Angew. Math. Phys.* **12**(2), 115–132 (1961).
7. R. M. Fand, Heat transfer by forced convection from a cylinder to water in crossflow, *Int. J. Heat Mass Transfer* **8**, 995–1010 (1965).
8. H. C. Perkins and G. Leppert, Forced convection heat transfer from a uniformly heated cylinder, *J. Heat Transfer* **84**, 257–261 (1962).
9. H. C. Perkins and G. Leppert, Local heat-transfer coefficients on a uniformly heated cylinder, *Int. J. Heat Mass Transfer* **7**, 143–158 (1964).
10. W. Z. Sadeh, S. P. Sutera and P. F. Maeder, An investigation of vorticity amplification in stagnation flow, Brown University *Tech. Rep.* No. AF 1754/4, WT 50 (January (1968).
11. J. Kestin, P. F. Maeder and H. E. Wang, On boundary layers associated with oscillating streams, *Appl. Scient. Res.* **A10**, 1–22 (1961).
12. K. Pearson, *Tables of the Incomplete Γ-Function.* H.M.O. London (1922).

Résumé—La sensibilité élevée du transport de chaleur au point d'arrêt en présence de la turbulence de l'écoulement amont a été attribuée à l'amplication de la corticité par étirement des filaments tourbillonnaires. Un modèle mathématique proposé par Sutera, Maeder et Kestin est examiné dans le cas d'un nombre de Prandtl (Pr) très élevé. Les solutions asymptotiques obtenues pour le cas limite $Pr \to \infty$ montrent que la sensibilité du transport de chaleur continue à croitre avec le nombre de Prandtl. 95 pour cent approximativement de la valeur asymptotique du coefficient de transport de chaleur au point d'arrêt est atteinte pour $Pr = 100$.

Zusammenfassung—Die grosse Empfindlichkeit des Wärmeübergangs am Staupunkt, für Freistromturbulenz, wird der Wirbelvergrösserung infolge der Ausdehnung der Wirbelfäden zugeschrieben. Ein von Sutera, Maeder und Kestin vorgeschlagenes mathematisches Modell wird für den Fall sehr grosser Prandtl-Zahl (Pr) überprüft. Asymptotische Lösungen erhält man für den Grenzfall $Pr \to \infty$. Sie zeigen, dass die Empfindlichkeit des Wärmeübergangs mit dem Anstieg der Prandtl-Zahl zunimmt. Etwa 95 prozent des asymptotischen Wertes des Wärmeübergangskoeffizienten am Staupunkt werden bei $Pr = 100$ erhalten.

Аннотация—Сильная чувствительность теплообмена в критической точке к наличию свободной турбулентности объясняется усилением завихренности из-за расширения вихревых нитей. Математическая модель, предложенная Сутера, Мэдером и Кестиным, проверялась для случая очень большого числа Прандтля (*Pr*). Получены асимптотические решения при $Pr \to \infty$. Они показывают, что чувствительность теплообмена возрастает с увеличением числа Прандтля. Примерно 95% асимптотического значения коэффициента теплообмена в критической точке получены при $Pr = 100$.